Heat Transfer in a Couple Stress Fluid over a Continuous Moving Surface with Internal Heat Generation and Convective Boundary Conditions

Tasawar Hayat[a,b], Zahid Iqbal[a], Muhammad Qasim[c], and Omar M. Aldossary[b]

[a] Department of Mathematics, Quaid-i-Azam University 45320, Islamabad 44000, Pakistan
[b] Department of Physics, Faculty of Science, King Saud University, P.O. Box. 1846, Riyadh 11320, Saudi Arabia
[c] Department of Mathematics, COMSATS Institute of Information Technology (CIIT), Park Road, Chak Shahzad, Islamabad 44000, Pakistan

Reprint requests to M. Q.; E-mail: mq_qau@yahoo.com

Z. Naturforsch. **67a,** 217 – 224 (2012) / DOI: 10.5560/ZNA.2012-0021
Received June 8, 2011 / revised November 2, 2011

This investigation reports the boundary layer flow and heat transfer characteristics in a couple stress fluid flow over a continuos moving surface with a parallel free stream. The effects of heat generation in the presence of convective boundary conditions are also investigated. Series solutions for the velocity and temperature distributions are obtained by the homotopy analysis method (HAM). Convergence of obtained series solutions are analyzed. The results are obtained and discussed through graphs for physical parameters of interest.

Key words: Heat Transfer; Couple Stress Fluid; Heat Generation; Convective Boundary Conditions; Moving Surface.

1. Introduction

There are several fluids in industry and biology which cannot be described by Newton's law of viscosity. Examples of such fluids are certain paints, polymer solutions, cosmetic, food products, etc. The diverse characteristics of such fluids leads to a motivation that these cannot be derived by a single constitutive relation between shear stress and shear rate. The constitutive equations of non-Newtonian fluids vary greatly in complexity and are of higher order than the Navier–Stokes equations. Despite of all the complications, the interest of the researchers in the flow of non-Newtonian fluids has grown (see [1 – 5]). The couple stress fluid theory developed by Stokes [6] represents the simplest generalization of the classical viscous fluid theory that sustains couple stresses and the body couples. The important feature of these fluids is that the stress tensor is not symmetric and their accurate flow behaviour cannot be predicted by the classical Newtonian theory. The main effect of the couple stresses will introduce a size dependent effect that is not present in the classical viscous theories. The fluids consisting of rigid, randomly oriented particles suspended in a viscous medium, such as blood, lubricants containing a small amount of polymer additive, electro-rheological fluids, and synthetic fluids are examples of these fluids [7]. Some more recent contributions which here taken into consideration the flows of couple stress fluid include Eldabe et al. [8], Mekheimer [9], Kumar and Singh [10], and Shantha and Shanker [11]. On the other hand, the boundary layer flows and heat transfer are useful in continuos casting, glass drawing, finite-fiber malts, paper production, insulating materials, etc. Sakiadis [12] started the seminal work on boundary layer flow over a moving surface with constant speed. Subsequently, such flows have been investigated extensively under various conditions. Hassanien [13] has investigated the non-Newtonian boundary layer flow of a power law fluid on a continuos moving flat plate in a parallel free stream. Magnetohydrodynamic (MHD) flow of a non-Newtonian fluid over a continuos moving surface with a parallel free stream was analyzed by Kumari and Nath [14]. Boundary layer flow of a micropolar fluid over a continuously moving permeable surface was studied numerically by Ishak et al. [15]. Hayat et al. [16] presented an analysis on the flow and heat

transfer over a continuously moving surface with a parallel free stream in a viscoelastic fluid. It is noticed from the existing literature that no investigation has been made so far to study the effect of heat generation in a non-Newtonian fluid over a moving surface with convective boundary conditions [17–20]. Hence the present attempt is made to present such study for the flow of a couple stress fluid. The homotopy analysis method (HAM) [21–28] is employed for the development of the series solutions. Such analysis even for a viscous fluid and without heat generation has not been reported yet.

2. Problem Statement

Consider the steady laminar boundary layer flow of an incompressible couple stress fluid over a surface moving with constant velocity u_w in the same direction as that of the uniform free stream velocity u_∞ (see physical model described in Figure 1). It is assumed that the wall and the free stream temperature, T_w and T_∞, are constants with $T_w > T_\infty$. The internal heat generation effects and convective boundary conditions are taken into account.The flow problem is governed by the following fundamental equations [6]:

$$\operatorname{div}\mathbf{V} = 0, \tag{1}$$

$$\rho\left[\frac{\partial \mathbf{V}}{\partial t} + (\mathbf{V}\cdot\nabla)\mathbf{V}\right] = -\nabla p - \mu(\nabla\times\nabla\times\mathbf{V}) - \eta(\nabla\times\nabla\times\nabla\times\nabla\times\mathbf{V}), \tag{2}$$

$$\rho C_p \frac{\mathrm{d}T}{\mathrm{d}t} = k\nabla^2 T, \tag{3}$$

where ρ is the fluid density, μ the dynamic viscosity, η the couple stress viscosity coefficient, T the fluid temperature, k the thermal conductivity, C_p the specific heat at constant pressure, and p the pressure; the viscous dissipation in the energy equation is neglected. By invoking the velocity field $\mathbf{V} = [u(x,y), v(x,y), 0]$, the boundary layer forms of above expressions give

$$\frac{\partial u}{\partial x} + \frac{\partial v}{\partial y} = 0, \tag{4}$$

$$u\frac{\partial u}{\partial x} + v\frac{\partial u}{\partial y} = \nu\frac{\partial^2 u}{\partial y^2} - \nu'\frac{\partial^4 u}{\partial y^4}, \tag{5}$$

$$u\frac{\partial T}{\partial x} + v\frac{\partial T}{\partial y} = \alpha\frac{\partial^2 T}{\partial y^2} + Q(T - T_\infty). \tag{6}$$

The boundary conditions are

$$\begin{aligned} &u = u_w,\ v = v_w,\ -k\frac{\partial T}{\partial y} = h_f(T_f - T) \\ &\text{at } y = 0, \\ &u \to u_\infty,\ \frac{\partial u}{\partial y} \to 0,\ T \to T_\infty \text{ as } y \to \infty. \end{aligned} \tag{7}$$

In above expressions $\nu = \mu/\rho$ denotes the kinematic viscosity, $\nu' = \eta/\rho$ the couple stress kinematic viscosity, h_f the convective heat transfer coefficient, T_f the convective fluid temperature below the moving sheet, α the thermal diffusitivity, and u and v are the velocity components parallel to the x- and y-axes, respectively. Defining

$$\begin{aligned} &u = Uf'(\xi),\ v = -\sqrt{\frac{U\nu}{2x}}\left[f(\xi) - \eta f'(\xi)\right], \\ &\xi = -\sqrt{\frac{U}{2x\nu}}y,\ \theta(\xi) = \frac{T - T_\infty}{T_f - T_\infty}, \end{aligned} \tag{8}$$

(4) is identically satisfied, and the other equations yield

$$f''' + ff'' - Kf^v = 0, \tag{9}$$

$$\theta'' + \Pr f\theta' + \lambda\Pr\theta = 0, \tag{10}$$

$$\begin{aligned} &f'(\xi) = r,\ f(\xi) = S,\ \theta'(\xi) = -\gamma(1 - \theta(\xi)) \\ &\text{at } \xi = 0, \\ &f'(\xi) \to 1 - r,\ f''(\xi) \to 0,\ \theta(\xi) \to 0 \\ &\text{as } \xi \to \infty. \end{aligned} \tag{11}$$

Here $U = u_w + u_\infty$; $f(0) = S$ with $S < 0$ corresponds to suction case and $S > 0$ implies injection; r is a ratio parameter, Pr the Prandtl number, γ the Biot number, K the couple stress parameter, and λ the heat generation

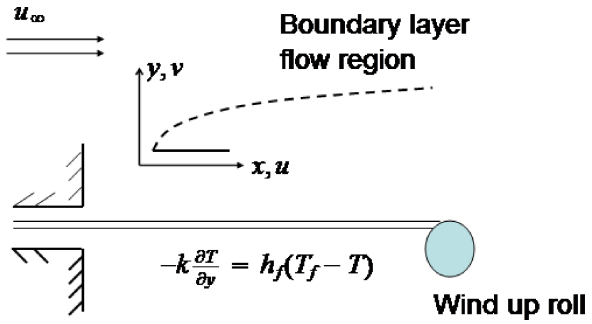

Fig. 1 (colour online). Physical flow model.

parameter. The definitions of these parameters are

$$r=\frac{u_{\mathrm{w}}}{U},\ \mathrm{Pr}=\frac{\upsilon}{\alpha},\ K=\frac{\eta U}{2\mu x v}, \tag{12}$$
$$\gamma=\frac{h_{\mathrm{f}}}{k}\sqrt{\frac{2vx}{U}},\ \lambda=\frac{2Qx}{U},\ S=-\left(\sqrt{\frac{2x}{vU}}\right)v_{\mathrm{w}}.$$

For $r=0$, we obtain the laminar boundary layer flow induced by a stationary surface (Blasius flow). However, we obtain the flow over a moving surface in absence of free stream velocity for $r=1$ (Sakiadis flow). If $r<0$, the free stream is directed toward the positive x-direction whereas the plate moves toward the negative x-direction, and prime shows differentiation with respect to ξ.

Expressions for the skin friction coefficient C_{f} and the local Nusselt number Nu_x are

$$C_{\mathrm{f}}=\frac{\tau_{\mathrm{w}}}{\rho},\ \mathrm{Nu}_x=\frac{xq_{\mathrm{w}}}{\alpha\left(T_{\mathrm{f}}-T_{\infty}\right)}, \tag{13}$$

or

$$\left(\mathrm{Re}_x\right)^{-1/2}C_{\mathrm{f}}=-f''(0), \tag{14}$$
$$\left(\mathrm{Re}_x\right)^{-1/2}\mathrm{Nu}_x=-\theta'(0), \tag{15}$$

where $\mathrm{Re}_x=Ux/\nu$ is the local Reynolds number.

3. Series Solutions

We express $f(\xi)$ and $\theta(\xi)$ in the set of base functions

$$\left\{\xi^k\mathrm{e}^{-n\xi}\,\middle|\,k\geq 0,n\geq 0\right\} \tag{16}$$

in the forms

$$f(\xi)=a^0_{0,0}+\sum_{n=0}^{\infty}\sum_{k=0}^{\infty}a^k_{m,n}\xi^k\mathrm{e}^{-n\eta}, \tag{17}$$
$$\theta(\xi)=b^0_{0,0}+\sum_{n=0}^{\infty}\sum_{k=0}^{\infty}b^k_{m,n}\xi^k\mathrm{e}^{-n\eta}, \tag{18}$$

where $a^k_{m,n}$ and $b^k_{m,n}$ are the coefficients. According to the rule of solution expressions for $f(\xi)$ and $\theta(\xi)$, and considering (9) and (10), the initial approximations and auxiliary linear operators are

$$f_0(\xi)=S+(1-2r)\left(1-\exp(-\xi)\right)+\lambda\xi,$$
$$\theta_0(\xi)=\frac{\gamma}{1+\gamma}\mathrm{e}^{-\xi}, \tag{19}$$
$$\mathcal{L}_f(f)=f'''-f',\ \mathcal{L}_\theta(f)=\theta''-\theta, \tag{20}$$

with

$$\mathcal{L}_f\left[A_1+A_2\mathrm{e}^{\xi}+A_3\mathrm{e}^{-\xi}\right]=0, \tag{21}$$
$$\mathcal{L}_\theta\left[A_4\mathrm{e}^{\xi}+A_5\mathrm{e}^{-\xi}\right]=0, \tag{22}$$

where A_i $(i=1-5)$ are the arbitrary constants. From (9) and (10), the nonlinear operators $\mathcal{N}_f$ and $\mathcal{N}_\theta$ are defined as

$$\begin{aligned}\mathcal{N}_f\left[\widehat{f}(\xi;q)\right]&=\frac{\partial^3\widehat{f}(\xi;q)}{\partial\xi^3}\\&+\widehat{f}(\xi;q)\frac{\partial^2\widehat{f}(\xi;q)}{\partial\xi^2}-K\frac{\partial^5\widehat{f}(\xi;q)}{\partial\xi^5},\\\mathcal{N}_\theta\left[\widehat{\theta}(\xi;q),\widehat{f}(\xi;q)\right]&=\frac{\partial^2\widehat{\theta}(\xi;q)}{\partial\xi^2}\\&+\mathrm{Pr}\,\widehat{f}(\xi;q)\frac{\partial\widehat{\theta}(\xi;q)}{\partial\xi}+\lambda\,\mathrm{Pr}\,\widehat{\theta}(\xi;q).\end{aligned} \tag{23}$$

In above expressions, $\widehat{f}(\xi;q)$ and $\widehat{\theta}(\xi;q)$ are the mapping functions for $f(\xi)$ and $\theta(\xi)$, respectively, where q is an embedding parameter in the range $[0,1]$. It is worth mentioning that $\widehat{f}(\xi,q)$ and $\widehat{\theta}(\xi,q)$ vary from $f_0(\xi)$ and $\theta_0(\xi)$ to the final solutions $f(\xi)$ and $\theta(\xi)$ when q varies from 0 to 1. The problems at the zeroth-order and nth-order deformations are as follows.

3.1. Zeroth-Order Problem

$$(1-q)\mathcal{L}_f\left[\widehat{f}(\xi;q)-f_0(\xi)\right]=q\hbar\mathcal{N}_f\left[\widehat{f}(\xi;q)\right], \tag{24}$$
$$\widehat{f}'(0;q)=r,\ \widehat{f}(0;q)=S,\ \widehat{f}'(\infty;q)=1-r,\ \widehat{f}''(\infty;q)=0, \tag{25}$$
$$\begin{aligned}&(1-q)\mathcal{L}_\theta\left[\widehat{\theta}(\xi;q)-\theta_0(\xi)\right]\\&\quad=q\hbar\mathcal{N}_\theta\left[\widehat{\theta}(\xi;q),\widehat{f}(\xi;q)\right],\end{aligned} \tag{26}$$
$$\widehat{\theta}'(0;q)=-\gamma\left(1-\widehat{\theta}(0;q)\right),\ \widehat{\theta}(\infty;q)=0. \tag{27}$$

3.2. nth-Order Deformation Problems

Differentiating the zeroth-order deformation equations (24) and (26) n times by the Leibnitz rule with respect to q, then dividing by $n!$, and finally setting $q=0$, we have

$$\mathcal{L}_f\left[f_n(\xi)-\chi_n f_{n-1}(\xi)\right]=\hbar_{\mathrm{f}}\mathcal{R}^f_n(\xi), \tag{28}$$
$$f'_n(0)=f_n(0)=f'_n(\infty)=0, \tag{29}$$

$$\mathcal{L}_\theta\left[\theta_n(\xi)-\chi_n\theta_{n-1}(\xi)\right]=\hbar_\theta\mathcal{R}_n^\theta(\xi), \tag{30}$$

$$\theta_n(0)=\theta_n'(\infty)-\gamma\theta_n(\infty)=0, \tag{31}$$

$$\mathcal{R}_n^f(\xi)=f_{n-1}'''(\xi)-Kf_{n-1}^v(\xi)+\sum_{k=0}^{n-1}f_{n-1-k}f_k''(\xi), \tag{32}$$

$$\mathcal{R}_n^\theta(\xi)=\theta_{n-1}''(\xi)+\lambda\,\mathrm{Pr}\,\theta_{n-1}(\xi)+\mathrm{Pr}\sum_{k=0}^{n-1}f_{n-1-k}(\xi)\,\theta_k'(\xi), \tag{33}$$

$$\chi_n=\begin{cases}0, & n\le 1,\\ 1, & n>1,\end{cases} \tag{34}$$

where $\hbar$ depicts a non-zero auxiliary parameter. When $q=0$ and $q=1$, then we get

$$\widehat{f}(\xi,0)=f_0(\xi),\ \ \widehat{f}(\xi,1)=f(\xi), \tag{35}$$

$$\widehat{\theta}(\xi,0)=\theta_0(\xi),\ \ \widehat{\theta}(\xi,1)=\theta(\xi). \tag{36}$$

In view of (35) and (36) and Taylor's theorem, one obtains

$$\widehat{f}(\xi,q)=f_0(\xi)+\sum_{n=1}^{\infty}f_n(\xi)\ q^n,\qquad f_n(\xi)=\frac{1}{n!}\frac{\partial^n\widehat{f}(\xi,q)}{\partial q^n}\bigg|_{q=0}, \tag{37}$$

$$\widehat{\theta}(\xi,q)=\theta_0(\xi)+\sum_{n=1}^{\infty}\theta_n(\xi)\ q^n,\qquad \theta_n(\xi)=\frac{1}{n!}\frac{\partial^n\widehat{\theta}(\xi,q)}{\partial q^n}\bigg|_{q=0}, \tag{38}$$

where the convergence of series (37) and (38) depends upon $\hbar$. One can make a choice of $\hbar$ so that the series (37) and (38) converge for $q=1$. Therefore,

$$f(\xi)=f_0(\xi)+\sum_{n=1}^{\infty}f_n(\xi), \tag{39}$$

$$\theta(\xi)=\theta_0(\xi)+\sum_{n=1}^{\infty}\theta_n(\xi). \tag{40}$$

The general solutions $f_n(\xi)$ and $\theta_n(\xi)$ in terms of the special solutions $f_n^\star(\xi)$ and $\theta_n^\star(\xi)$ are

$$f_n(\xi)=f_n^\star(\xi)+A_1+A_2\,\mathrm{e}^{\xi}+A_3\,\mathrm{e}^{-\xi}, \tag{41}$$

$$\theta_n(\xi)=\theta_n^\star(\xi)+A_4\,\mathrm{e}^{\xi}+A_5\,\mathrm{e}^{-\xi}. \tag{42}$$

Here $A_i\ (i=1-5)$, subject to the conditions (29) and (31), are

$$A_2=A_4=0,\ \ A_3=\frac{\partial f_n^\star(\xi)}{\partial\xi}\bigg|_{\xi=0},\qquad A_1=-A_3-f_n^\star(0),\qquad A_5=\frac{1}{1+\gamma}\left(\theta_n^{\star\prime}(\xi)|_{\xi=0}-\gamma\theta_n^\star(\eta)|_{\xi=0}\right). \tag{43}$$

It should be pointed out that the problems consisting of (28)–(34) are solved by using the symbolic computation software Mathematica for $n=1,2,3,\ldots$

4. Convergence of the Series Solutions

It is well known that the homotopic procedure leads to a series solution. The convergence analysis of this series solution is quite important. Therefore we plotted $\hbar$-curves for this objective and present Figure 2 in this direction. This figure depicts that ranges for permissible values of $\hbar_{\mathrm{f}}$ and $\hbar_\theta$ are $-1.0\le\hbar_{\mathrm{f}}\le-0.25$ and $-1.3\le\hbar_\theta\le-0.25$. Further, for $\hbar_{\mathrm{f}}=\hbar_\theta=-0.75$, we obtain convergent series solutions in the whole region of ξ.

5. Results and Discussion

In this section, we discuss the influence of the various parameters γ, K, S, r, Pr, and λ on velocity $f'(\xi)$ and temperature field $\theta(\xi)$. For this aim, we plotted Figures 2–11. Figure 3 illustrates the effect of various values of the velocity ratio parameter r on the velocity field $f'(\xi)$. It is observed that the velocity decreases

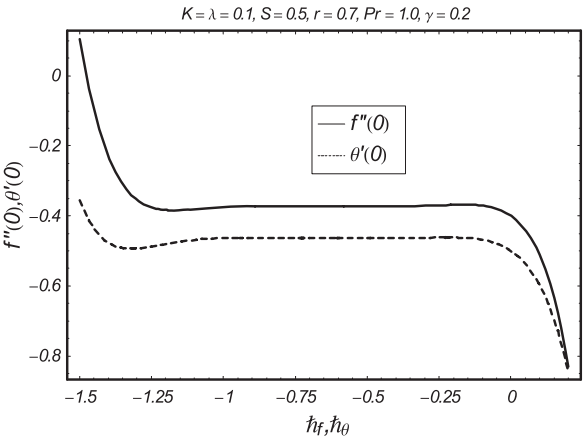

Fig. 2. $\hbar$-curve for 20th-order of approximation.

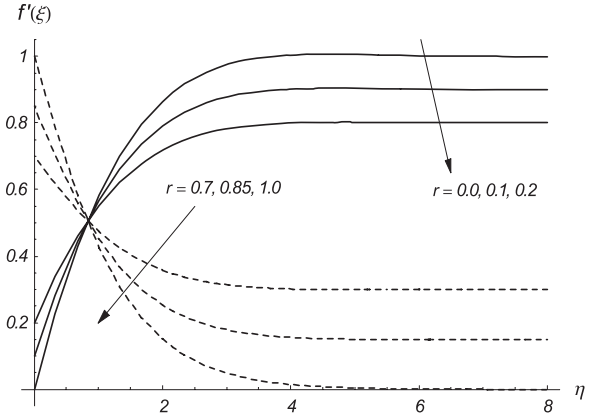

Fig. 3. Influence of ratio parameter r on f' when $K = 0.1$, $S = 0.5$.

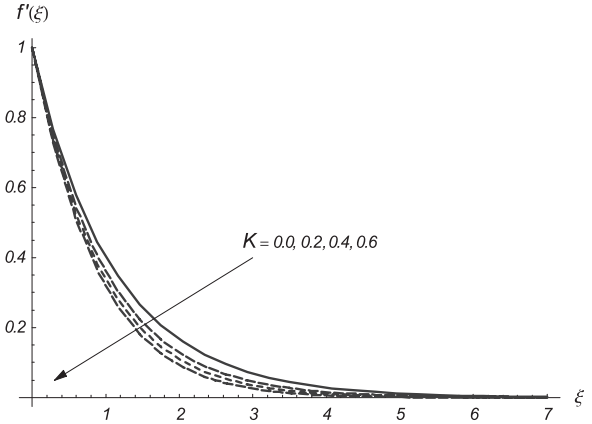

Fig. 4. Influence of couple stress parameter K on f' when $r = 1.0$, $S = 0.5$.

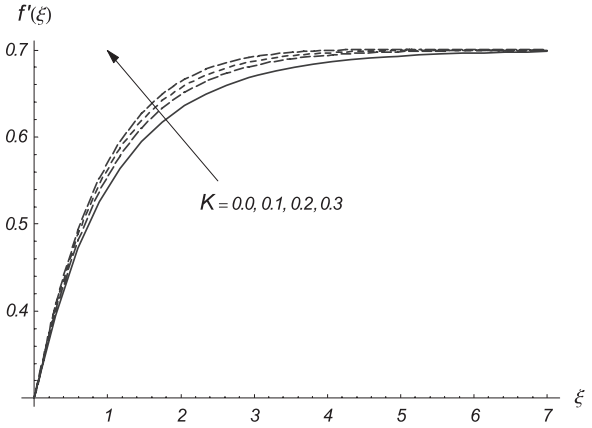

Fig. 5. Influence of couple stress parameter K on f' when $r = 0.3$, $S = 0.5$.

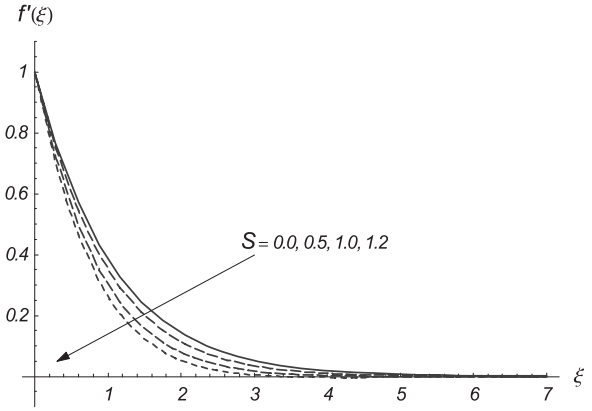

Fig. 6. Influence of suction parameter S on f' when $r = 1.0$, $K = 0.1$.

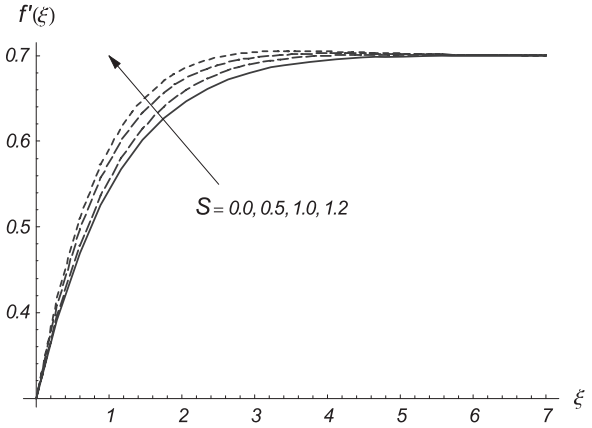

Fig. 7. Influence of suction parameter S on f' when $r = 0.3$, $K = 0.1$.

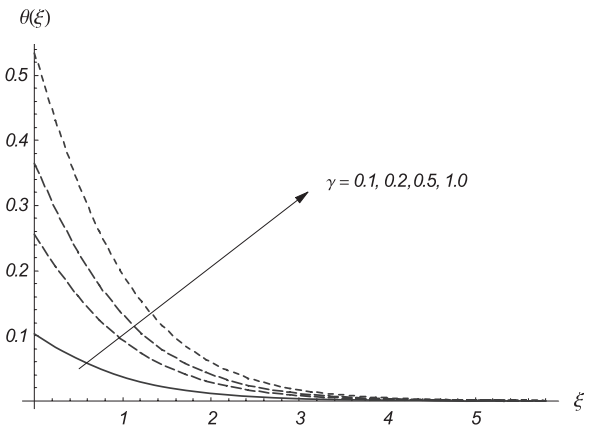

Fig. 8. Influence of Biot number γ on θ when $r = 0.7$, $K = 0.1$, $\mathrm{Pr} = 1.0$, $S = 0.5$, $\lambda = 0.2$.

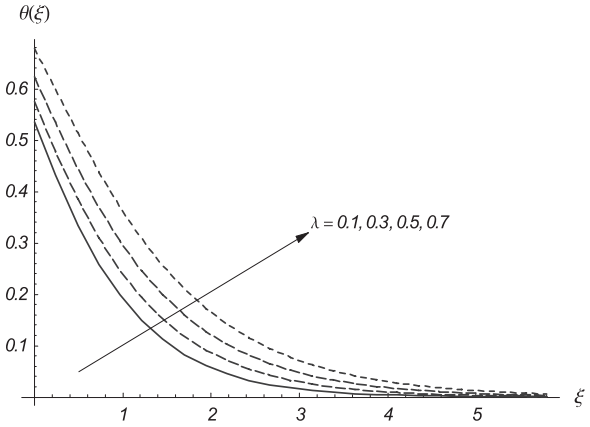

Fig. 9. Influence of heat generation parameter λ on θ when $r = 0.7$, $K = 0.1$, $\gamma = 1.0$, $S = 0.5$, $\Pr = 0.1$.

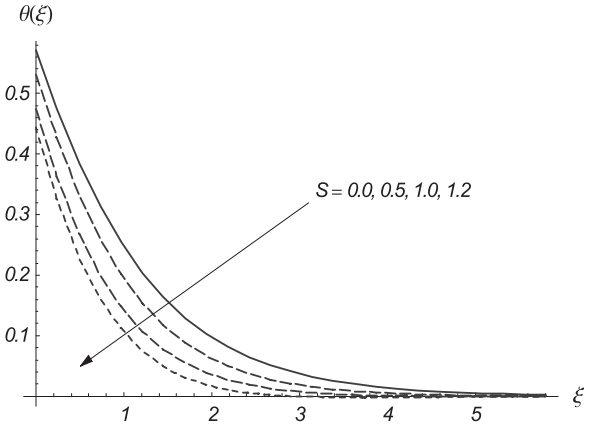

Fig. 10. Influence of suction parameter S on θ when $r = 0.7$, $K = 0.1$, $\Pr = 1.0$, $\gamma = 1.0$, $\lambda = 0.2$.

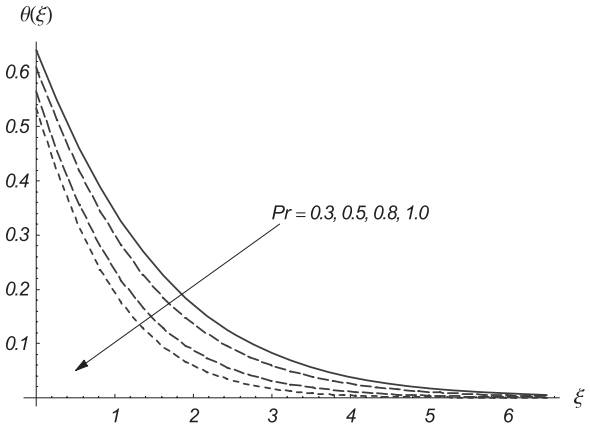

Fig. 11. Influence of Prandtl number Pr on θ when $r = 0.7$, $K = 0.1$, $S = 0.5$, $\gamma = 1.0$, $\lambda = 0.2$.

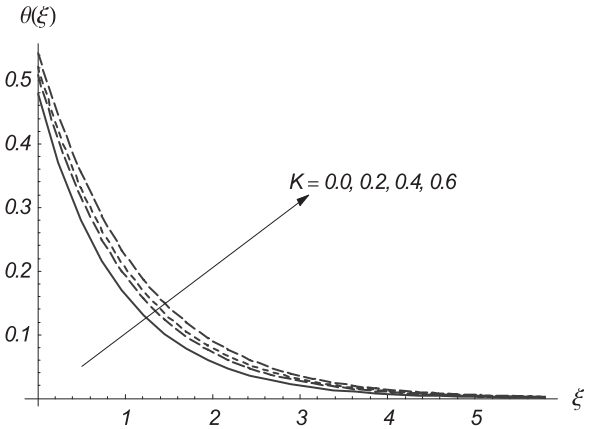

Fig. 12. Influence of couple stress parameter K on θ when $r = 0.7$, $K = 0.1$, $\Pr = 1.0$, $\gamma = 1.0$, $S = 0.5$, $\lambda = 0.2$.

and the boundary layer thickness increases with an increase in r $(0 \leq r < 0.5)$ whereas both velocity and the boundary layer thickness are decreasing functions of r $(r > 0.5)$. From physical point of view $0 \leq r < 0.5$ is the case when the plate and the fluid are moving in the same direction. If $r > 1$, the free stream is directed towards the positive x-direction, while the plate moves towards the negative x-direction. On the other hand, if $r < 1$, the free stream is directed upwards the negative x-direction, while the plate moves towards the positive x-direction. Figures 4 and 5 depict the effect of K on $f'(\xi)$ for different values of r. From Figure 4, for fixed $r = 1$ (Sakiadis flow), we noticed that the velocity profile decreases by increasing K and the boundary layer thickness decreases slightly with an increase in K. It is obvious from Figure 5 that the velocity increases with the increasing values of K when $r = 0.3$. The effect of the suction parameter S on $f'(\xi)$ has been illustrated in Figures 6 and 7 for different values of r. From Figure 6 for fixed $r = 1$ (Sakiadis flow), the velocity and

Table 1. Convergence of the homotopy solutions for different orders of approximation when $K = 0.1$, $\lambda = 0.2$, $\Pr = 1.0$, $r = 0.7$, $S = 0.5$, $\gamma = 0.6$, and $\hbar_f = \hbar_\theta = -0.6$.

Order of approximation	$f''(0)$	$-\theta'(0)$
5	0.154126	0.363669
10	0.150662	0.346649
15	0.150622	0.343879
20	0.150636	0.343487
25	0.150645	0.343432
30	0.150645	0.343432

boundary layer thickness are decreasing functions of S. It is clear from Figure 7 that the velocity increases with the increasing values of S when $r = 0.3$. Physically, sucking the fluid particles through porous wall reduce the growth of the boundary layer. This is quite compatible with the fact that suction causes reduction in boundary layer thickness. Hence, a porous character of the wall provides a powerful mechanism for controlling the momentum boundary layer thickness. Figure 8 represented the effect of the Biot number γ on $\theta(\xi)$. It is obviously from Figure 8 that both temperature $\theta(\xi)$ and thermal boundary layer thickness increase with an increasing in γ. For fixed cold fluid properties and for fixed free stream velocity, γ at any location x is directly proportional to the transfer coefficients associated with the hot fluid, namely h_{f}. Now the resistance on the hot fluid is inversely proportional to h_{f}. Thus when γ increases then the hot fluid convection resistance decreases and consequently the temperature increases (see [17]). The effects of λ on $\theta(\xi)$ have been portrayed in Figure 9. We conclude that γ and λ have the same qualitative effects on the temperature profile $\theta(\xi)$. An increase in the suction parameter S corresponds to a decrease in the temperature and the thermal boundary layer thickness (see Fig. 10). The effect of the Prandtl number Pr on $\theta(\xi)$ can be visualized in Figure 11. It is obvious that an increase in the values of Pr greatly reduces the thermal diffusivity, therefore temperature and the thermal boundary layer thickness are decreasing functions of Pr. It is also observed that the deviation in the temperature profiles are more significant for small values of Pr when compared with its larger values. It is important to note that Pr (< 1) corresponds to liquid metals which have higher thermal diffusivity, while large values of Pr (> 1) lead to high-viscosity oils. To gain insight towards the behaviour of couple stress parameter K on the temperature field, we display Figure 12. The larger values of K significantly increase the temperature and thermal boundary layer thickness. Table 1 analyzes the convergence of the series solution. It is observed that convergence for the functions f and θ are achieved at only 20th-order of approximations.

6. Summary

In this work, we studied the steady flow of a couple stress fluid over a moving surface in the presence of internal heat generation and convective boundary conditions. The main points of the present study are as follows:

- The couple stress parameter K decreases the boundary layer thickness.
- The temperature profile $\theta(\xi)$ increases in view of an increase in λ and γ.
- The Prandtl number Pr leads to a decrease in $\theta(\xi)$.
- The effect of K on the velocity $f'(\xi)$ and temperature $\theta(\xi)$ are qualitatively similar.

Acknowledgement

Prof. Hayat as a visiting professor very much thanks the King Saud University through the support (KSU-VPP-117).

[1] S. Wang and W. C. Tan, Phys. Lett. A **372**, 3046 (2008).
[2] C. Fetecau, M. Athar, and C. Fetecau, Comput. Math. Appl. **57**, 596 (2009).
[3] T. Hayat, M. Awais, M. Qasim, and A. Hendi, Int. J. Heat Mass Transfer **54**, 3777 (2011).
[4] T. Hayat and M. Qasim, Z. Naturforsch. **65a**, 950 (2010).
[5] S. Asghar, T. Hayat, and P. D. Ariel, Commun. Nonlinear Sci. **14**, 154 (2009).
[6] V. K. Stokes, Phys. Fluids **9**, 1709 (1966).
[7] D. Srinivasacharya, N. Srinivasacharyulu, and O. Odelu, Int. Commun. Heat Mass **36**, 180 (2009).
[8] N. T. M. Eldabe, A. A. Hassan, and M. A. A. Mohamed, Z. Naturforsch. **58a**, 204 (2003).
[9] K. S. Mekheimer, Biorheology **39**, 755 (2002).
[10] R. Kumar and M. Singh, Z. Naturforsch. **64a**, 448 (2009).
[11] G. Shantha and B. Shanker, Int. J. Numer. Method H. **20**, 250 (2010).
[12] B. C. Sakiadis, AIChE J. **7**, 221 (1961).
[13] I. A. Hassanien, Appl. Math. Model. **20**, 779 (1996).
[14] M. Kumari and G. Nath, Acta Mech. **146**, 139 (2001).
[15] A. Ishak, R. Nazar, and I. Pop, Int. J. Heat Mass Transfer **50**, 4743 (2007).
[16] T. Hayat, Z. Abbas, and I. Pop, Numer. Meth. Part. D. E. **26**, 305 (2010).
[17] A. Ishak, Appl. Math. Comput. **217**, 837 (2010).
[18] A. Aziz, Commun. Nonlinear Sci. **14**, 1064 (2009).
[19] A. Aziz, Commun. Nonlinear Sci. **15**, 573 (2010).
[20] O. D. Makinde and P. O. Olanrewaju, ASME J. Fluid Eng. **132**, 044502-2 (2010).
[21] S. J. Liao, Beyond Perturbation: Introduction to Homotopy Analysis Method, Chapman and Hall, CRC Press, Boca Reton 2003.

[22] S. J. Liao, Commun. Nonlinear Sci. **14**, 983 (2009).
[23] T. Hayat, M. Qasim, and Z. Abbas, Commun. Nonlinear Sci. **15**, 2375 (2010).
[24] S. Abbasbandy and E. Shivanian, Commun. Nonlinear Sci. **15**, 3830 (2010).
[25] T. Hayat, M. Qasim, and Z. Abbas, Z. Naturforsch. **65a**, 231 (2010).
[26] A. S. Bataineh, M. S. M. Noorani, and I. Hashim, Commun. Nonlinear Sci. **14**, 409 (2009).
[27] A. S. Bataineh, M. S. M. Noorani, and I. Hashim, Phys. Lett. A **372**, 4062 (2008).
[28] T. Hayat, M. Qasim, and Z. Abbas, Commun. Nonlinear Sci. **15**, 2375 (2010).